

The role of dynamics on the habitability of an Earth-like planet

ELKE PILAT-LOHINGER

Institute of Astrophysics, University of Vienna,
Türkenschanzstrasse 17, A-1180 Vienna, Austria

Abstract

From the numerous detected planets outside the Solar system, no terrestrial planet comparable to our Earth has been discovered so far. The search for an Exo-Earth is certainly a big challenge which may require the detections of planetary systems resembling our Solar system in order to find life like on Earth. However, even if we find Solar system analogues, it is not certain that a planet in Earth position will have similar circumstances as those of Earth. Small changes in the architecture of the giant planets can lead to orbital perturbations which may change the conditions of habitability for a terrestrial planet in the habitable zone (HZ). We present a numerical investigation where we first study the motion of test-planets in a particular Jupiter-Saturn configuration for which we can expect strong gravitational perturbations on the motion at Earth position according to a previous work. In this study, we show that these strong perturbations can be reduced significantly by the neighboring planets of Earth. In the second part of our study we investigate the motion of test-planets in inclined Jupiter-Saturn systems where we analyze changes in the dynamical behavior of the inner planetary system. Moderate values of inclination seem to counteract the perturbations in the HZ while high inclinations induce more chaos in this region. Finally, we carry out a stability study of the actual orbits of Venus, Earth and Mars moving in the inclined Jupiter-Saturn systems for which we used the Solar system parameters. This study shows that the three terrestrial planets will only move in low-eccentric orbits if Saturn's inclination is $\leq 10^\circ$. Therefore, it seems that it is advantageous for the habitability of Earth when all planets move nearly in the same plane.

Keywords: Planetary systems – Planets: Jupiter-Saturn – habitable zone

1 Introduction

The search for planets outside the Solar system has shown an unexpected diversity of planetary systems. Strange new worlds like pulsar planets, hot-Jupiters and high eccentricity motion of planets as well as planets in binary star systems were not expected by astronomers when starting their search for other worlds. The diversity of planetary systems is evidence that phases of instability during the formation process have shaped these systems. Numerical simulations, which showed hypothetical scenarios for the evolution of the Solar system – like e.g. the Nice models (Tsiganis et al. 2003, Morbidelli et al. 2009, Levison et

al. 2011) – indicated chaos in the orbital motion of the outer planetary system before the final architecture was reached. The strength and duration of this turbulent phase could be important for the future evolution of a planetary system, as different evolutionary tracks for the planetary motion will lead to different final architectures of a system.

The fact that the Solar system planets move in nearly the same plane and in nearly circular orbits could allude that the instability phase in our planetary system was moderate and, therefore, advantageous for the habitability of our Earth which is still the only planet known where life as we know it, exists. Taking into account that complex life on Earth needed an evolution over a very long time, we assume that the low-eccentricity and quite stable planetary motion might be a necessary requirement for “Earth-like” habitability. Therefore, the planet has to move in the so-called habitable zone (HZ) which is the region around the star where liquid water is stable on the surface of an Earth-type planet (Kasting et al. 1993)¹. In this study, we assume that the planet has one Earth ocean of surface water, where the carbonate-silicate cycle controls the CO₂ level in equilibrium with a temperature above the freezing in the HZ.

Therefore, we define the boundaries of the HZ to be at 0.95 au and 1.37 au, where the inner border is determined by the runaway greenhouse effect according to the work by Leconte et al. (2013) and the outer boundary is taken from Kasting et al. (1993)². We studied the dynamical behavior in this area via long-term computations of a set of test-planets moving in Sun-Jupiter-Saturn like configurations. Numerical stability studies of planetary motion in the HZ have been carried out since the detection of the first extra-solar planet by Mayor & Queloz in 1995. These studies examined the stability or formation of certain detected extra-solar planetary systems in single and multiple star systems. The first relevant publications are e.g. Gehman et al. (1996), Jones & Sleep (2002), Menou & Tabachnik (2003), Jones et al. (2005) and many others³ (see e.g. Sándor et al. (2007), Eggl et al. (2012, 2013), Müller & Haghighipour (2014)) whose general numerical studies can be applied to many of the discovered systems.

The present numerical study was motivated by previous investigations of Pilat-Lohinger et al. (2008a& b – hereafter PL08a and PL08b) which showed that strong secular perturbations act on the motion of test-planets in the HZ which can lead to high eccentricities for certain orbits (see the arched band in Fig. 2 in PL08a). Here, we focus on the region where secular perturbations affect the motion of an Earth-like planet at 1 au. This is the case when Saturn’s semi-major axis is 8.7 au. Then the motion of a terrestrial planet at 1 au would vary from nearly circular to highly eccentric (with an eccentricity ≥ 0.6). Consequently, the orbit will either be entirely, mostly, or only in average within

¹Besides this basic requirement many other conditions of astrophysical, geophysical, chemical and biological nature have to be fulfilled that a planet can be considered as habitable planet.

²This outer boundary does not take into account CO₂ clouds which can significantly affect the temperature-CO₂ coupling. These effects may shift the outer boundary to 1.7 au or 2 au (see e.g. Forget & Pierrehumbert, 1997 or Mischna et al., 2000).

³Unfortunately the literature is too rich on this subject to cite all relevant articles here.

the HZ.⁴ An orbit with eccentricity ≥ 0.6 would certainly belong to the latter case which would lead to strong variations in the surface temperature as shown by Williams & Pollard (2002) for Earth. In their study, these authors increased the eccentricity of Earth up to 0.7 and showed that Earth can stay habitable as the planet did not freeze out at its aphelion distance, and no complete water evaporation occurred at its perihelion distance.

Because the studies PL08a and PL08b have shown that the dynamical behavior in the HZ can change significantly when we modify the architecture of the system, we checked the influence of the ice-planets Uranus and Neptune and of the neighboring planets Venus and Mars in this particular Jupiter-Saturn system. Our study shows that especially Venus plays an important role (as it was also found in PL08a).

In the second part of this study, we considered inclined Jupiter-Saturn configurations for which we increased Saturn’s inclination up to 50° . The numerical simulations showed that systems with inclinations between 10° and 40° indicate a significant decrease in the maximum eccentricity for the test-planets in the HZ. And for higher inclinations the chaotic area increased.

Finally, we were interested in the dynamical behavior of the terrestrial planets Venus, Earth and Mars when moving in the inclined Jupiter-Saturn systems. These computations showed chaotic perturbations and an escape of Mars for an inclination of 20° for Saturn’s orbit. For higher inclinations, the orbit of Mars immediately becomes chaotic and perturbs the motion of Earth and Venus, as well. Moreover, the chaotic area increases with Saturn’s inclination.

This paper is organized as follows. We describe the perturbations in a planetary system in section 2, and present the computations in section 3. The study in a particular planar Jupiter-Saturn system is shown in section 4, and in the inclined Jupiter-Saturn configurations in section 5. Finally, in section 6, we examine the motion of the actual orbits of Venus, Earth and Mars in the inclined Jupiter-Saturn configurations.

2 Perturbations in a Planetary System

Planetary orbits are described by a set of orbital elements where the semi-major axis a and the eccentricity e define the size and the shape of the orbit and the angles: inclination i , argument of perihelion ω and longitude of the ascending node Ω specify the orientation of the orbit in space. Finally, the mean anomaly M defines the orbital position of the body. As soon as more than one planet is orbiting a star, there will be a variation of these orbital parameters due to gravitational interactions between the planets. From studies of the Solar system, we know that resonant perturbations may influence the orbital motion significantly. For our study the mean motion resonances (also known as orbital resonances) and secular resonances are of special interest.

Mean motion resonances (MMRs) occur when the orbital periods of two celestial bodies are close to a ratio of small integers

⁴This is similar to the classification of different HZs for binary star systems where between (i) permanent, (ii) extended and (iii) averaged HZs is distinguished (see Eggl et al., 2012).

$$\frac{n_1}{n_2} \sim \frac{k_1}{k_2}, \quad (1)$$

where n_1 and n_2 are the mean motions ($= \text{Orbital Period}/2\pi$) of the celestial bodies and k_1, k_2 are integers. Orbital resonances are the source of both stability and chaos, depending sensitively upon parameters and initial conditions. Well known examples of MMRs in the Solar system are the so-called Kirkwood gaps in the asteroid belt. The locations of these gaps correspond to MMRs with Jupiter.

Secular resonances (SR) occur when one of the precession frequencies of a celestial body – related to the motion of ω or Ω – is equal (or a linear combination) of the proper modes of the planetary motion (g_l, s_l with $l = 1, \dots, N$ where N is the number of planets – for the Solar System $l = 1$ corresponds to Mercury \dots $l = 8$ is Neptune). When considering the giant planets Jupiter and Saturn moving on low inclination and low eccentricity orbits, these frequencies can be deduced by the following secular linear approximation (see e.g. Murray & Dermott 1999)

$$\begin{aligned} g &= \frac{n}{4} \left(\frac{m_J}{m_{\text{Sun}}} \alpha_J^2 b_{3/2}^{(1)}(\alpha_J) + \frac{m_S}{m_{\text{Sun}}} \alpha_S^2 b_{3/2}^{(1)}(\alpha_S) \right) \\ s &= -g \end{aligned} \quad (2)$$

where $\alpha_J = a/a_J$, $\alpha_S = a/a_S$ with a_J, a_S, a_{TP} being the semi-major axes of Jupiter, Saturn and the test-planet, respectively. The quantities m_J and m_S are the masses of Jupiter and Saturn, m_{Sun} is the mass of the Sun and $b_{3/2}^{(1)}$ is a Laplace coefficient. Moreover, the test-planets are considered to be mass-less compared to the other masses and they must have nearly zero eccentricities and inclinations. Solutions of Eq. 2 for $g(a_{TP}, a_S) = g_5(a_S)$ and $g(a_{TP}, a_S) = g_6(a_S)$ are SRs connected to Jupiter or Saturn, respectively.

It is well known that SR and low order MMRs may lead to significant changes in the orbital motion of bodies with large variations in their eccentricities. This could cause problems for a planet in the HZ, which is a quite small region. If this planet moves in a high eccentricity orbit, it will leave the HZ periodically, which might change the conditions for it habitability.

3 Dynamical Model and Computations

To study the dynamics of test-planets in the HZ between 0.95 au and 1.37 au, we used the restricted problem which is commonly used for such investigations. The test-planet is considered to be mass-less and move in the gravitational field of the Sun, Jupiter and Saturn without perturbing their orbits.

In the first part of this study, Jupiter was fixed to its actual orbit at 5.2 au and Saturn's semi-major axis was changed to 8.7 au while the other orbital elements were those of the Solar system (as published in PL08a, Table 1). For the integrations, the Bulirsch-Stoer integration method was used and the

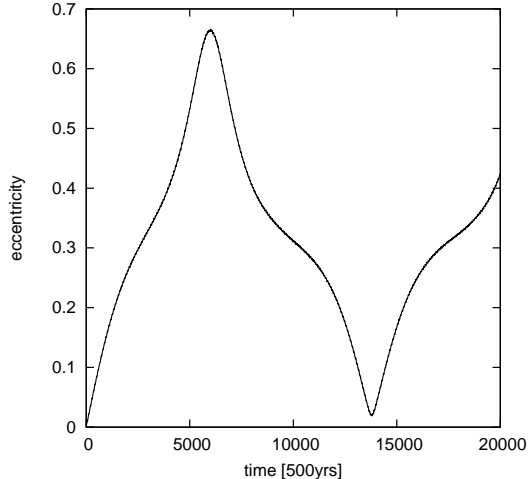


Figure 1: Time evolution of the eccentricity of a test-planet at 1 au for Saturn at 8.7 au.

stability of the orbital motion was verified calculating the Fast Lyapunov Indicator (FLI). This chaos indicator was introduced by Froeschlé et al. (1997) and is based on the Lyapunov Characteristic Exponent (LCE) (see e.g. Froeschlé, 1984). When calculating the FLI, one can easily distinguish between regular and chaotic motion due to the growth of the largest tangent vector of the dynamical flow. The growth can be either linear or exponential where the latter characterizes chaotic motion.

In the second part, we studied inclined Jupiter-Saturn systems for which we used the hybrid integration method of the Mercury6 package (Chambers, 1999). For the computation of the maximum eccentricity maps we took again the initial conditions published in PL08a and varied the inclination of Saturn from 10° to 50° in steps of 10° .

Finally, in the third part we examined the stability of the terrestrial planets (Venus to Mars) in the different inclined Jupiter-Saturn systems for which we used the orbital parameters of the Solar system.

4 The planar Jupiter-Saturn system

In PL08a, the locations of the two main secular frequencies associated with the precession of perihelia of Jupiter and Saturn (known as g_5 and g_6 frequencies in the Solar system) were calculated using the frequency analysis of Laskar (1990; see also Robutel & Gabern 2006). The result of $g = g_5$ (when applying Eq. 2) was found to be in good agreement with the arched band of higher eccentricity shown in Fig. 2 of PL08a. Due to this perturbation, the motion of a test-planet at 1 au indicates strong variations in eccentricity if Saturn orbits the Sun at 8.7 au. In Fig. 1, one can see a long periodic variation of the eccentricity which changes from circular to highly eccentric ($e > 0.6$) within 3 Myrs. Taking 0.95

au and 1.37 au as HZ boundaries, the entire orbit of this planet is in the HZ for only the first and last 150000 yrs of the 7 Myrs. For $0.05 < e < 0.4$, the planet is in the HZ for most of the time and leaves this zone only at peri-center. In case of $e > 0.4$, the planet exits the HZ at peri- and apo-center as it can be seen in Fig. 2. In this figure, one can see that less than 23% of the orbit of a planet with eccentricity of 0.7 (black line) would be in the HZ. However, a study by William and Pollard (2002) showed that Earth remains habitable even for such a high eccentricity. Of course, there would be strong variations of the surface temperature and then, probably the evolution of life would have been different to ours. If we shift the outer border to 1.67 au⁵ then the planet at 1 au leaves the HZ only when approaching the peri-center for all eccentricities > 0.05 and about 70% of a highly eccentric orbit ($e = 0.7$) would be in the HZ.

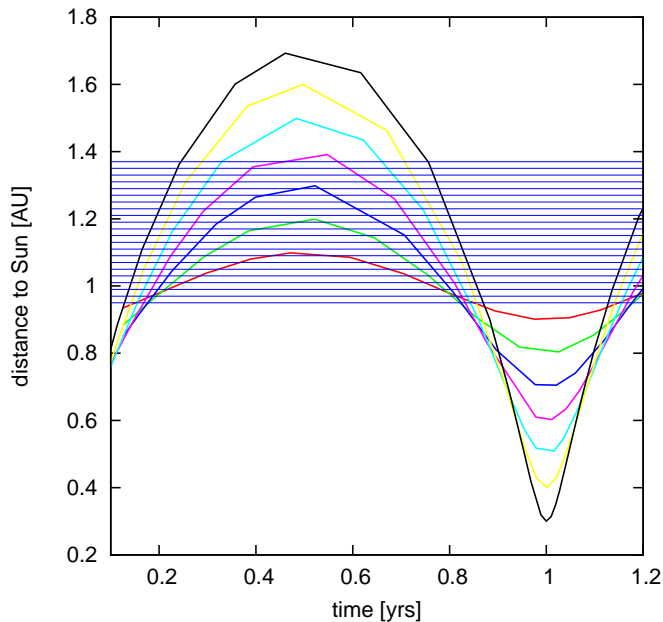


Figure 2: Distance to the Sun of a planet at 1 au. Each curve shows the variation of the distance over one orbital period of the planet using different orbital eccentricities represented by the different colors: 0.1 (red), 0.2 (green), 0.3: (blue), 0.4 (magenta), 0.5 (light blue), 0.6 (yellow) and 0.7 (black). The blue area labels the HZ.

Regardless of the choice of the HZ borders we recognized a difference between orbits with moderate ($e < 0.4$) and high eccentricities ($e \geq 0.4$) from the dynamical point of view. For the latter, small perturbations occur in semi-major axis (a), inclination (i) and ascending node (Ω) (see Figs. 3 a-c) whenever the planet's eccentricity exceeds 0.4. The strongest fluctuations appear when the orbit reaches its maximum eccentricity after 3 Myrs (see also Fig. 1). Moreover, the evolution of the planet's node (Fig. 3 bottom) shows transitions between

⁵When taking the maximum greenhouse effect as limit

rotation and libration when $e > 0.4$, which is known to be an indication of chaos.

To verify this orbital behavior, a long-term computation of the system over 100 Myrs has been performed where we also calculated the Fast Lyapunov Indicator (FLI) to determine the dynamical state of the orbit via this chaos indicator. In Fig. 4, one can see that the continuation of the simulation of Fig. 1 to longer times immediately points to a long period of high-eccentricity motion. More precisely, for more than 42 Myrs, the planet’s eccentricity is almost always in the range ≥ 0.4 , where chaos may arise. This can be seen clearly in Fig. 5 where the FLI of the planetary orbit increases whenever the eccentricity reaches its maximum value. This leads to a step-like increase of the FLI. Between 12 Myrs and 55 Myrs, when the eccentricity is almost always ≥ 0.4 , the curve has a steeper rise.

It is important to note that this study was carried out for a particular Jupiter-Saturn configuration. To generalize the results, we computed the orbital evolution using different relative positions of Jupiter and Saturn by varying Saturn’s mean anomaly and the argument of peri-center (see Fig. 6). As an indicator for dynamical habitability, we used the maximum eccentricity (max-e) which shows whether peri- and apo-center distance are in the HZ. Together with the evolution of the eccentricity, we can estimate if the orbit is permanently, mostly, or in average in the HZ (which depends also on the choice of the HZ borders). Moreover, the eccentricity indicates changes due to secular perturbations as shown in PL08a and PL08b. Fig. 6 shows the max-e values of a test-planet at 1 AU for different starting positions of Saturn (x-axis) and different orientations of Saturn’s orbit (y-axis). The color purple shows constellations of lowest max-e values and yellow corresponds to highest values of max-e. According to this map, one can see that the different Jupiter-Saturn configurations indicate mainly high values of maximum eccentricities (i.e. red, orange and yellow areas) and only a few configurations show moderate values of max-e between 0.2 and 0.35. This is the case when the relative values of both, the mean motions and the peri-centers are around 180° . The latter can also be zero according to Fig. 6. Only for these few combinations of the giant planets (i.e. blue and purple squares in Fig. 6), the test-planet at 1 au has low eccentricities so that the conditions for habitability could be quite similar to that of our Earth.

The planetary system studied here is much simpler than the Solar system as we took into account only two giant planets. For a better comparison with the Solar system, we studied the influence of Uranus, Neptune and the neighboring planets of Earth by including these planets in the dynamical model step by step. The results are shown in Fig. 7 where the red line represents the evolution of the test-planet’s eccentricity when using Jupiter through Neptune as dynamical model. The two ice planets do not decrease the maximum eccentricity significantly as the signal shows still a periodic variation in eccentricity (between 0 and 0.6) but with a different period. If we add Mars to the system, the test-planet’s eccentricity will be reduced to < 0.3 (see the green line in Fig. 7). However, the most important effect can be recognized when we include Venus. This planet damps the eccentricity of the test-planet at 1 au down to nearly

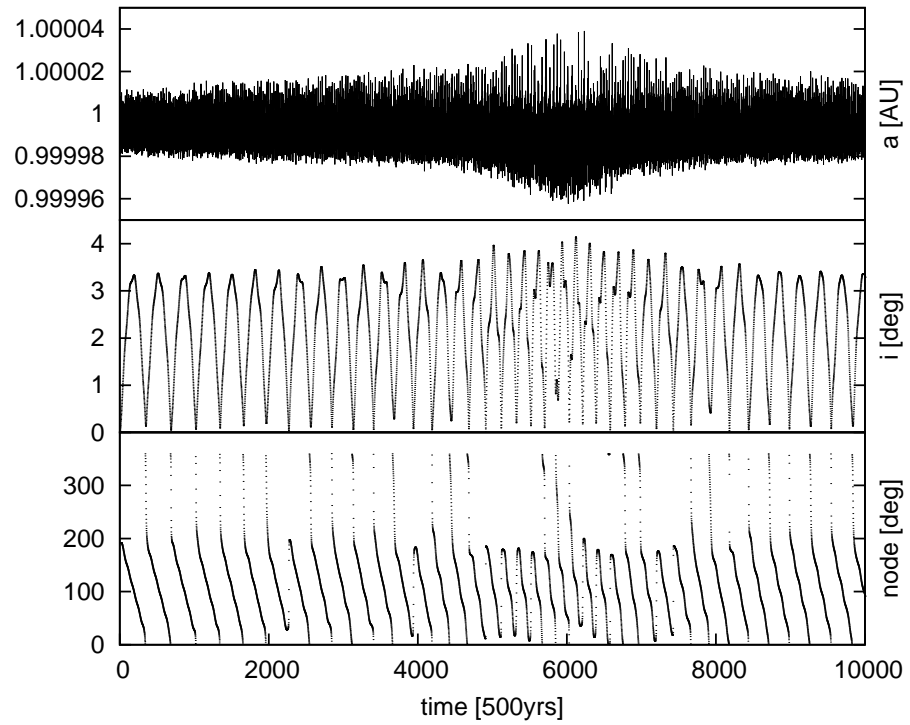


Figure 3: Time evolution of the semi-major axis a (top), the inclination i (middle) and the node (bottom) of the planetary orbit when its eccentricity exceeds 0.4. One can see small fluctuations in the top and middle panels and transitions between libration and circulation in the bottom panel.

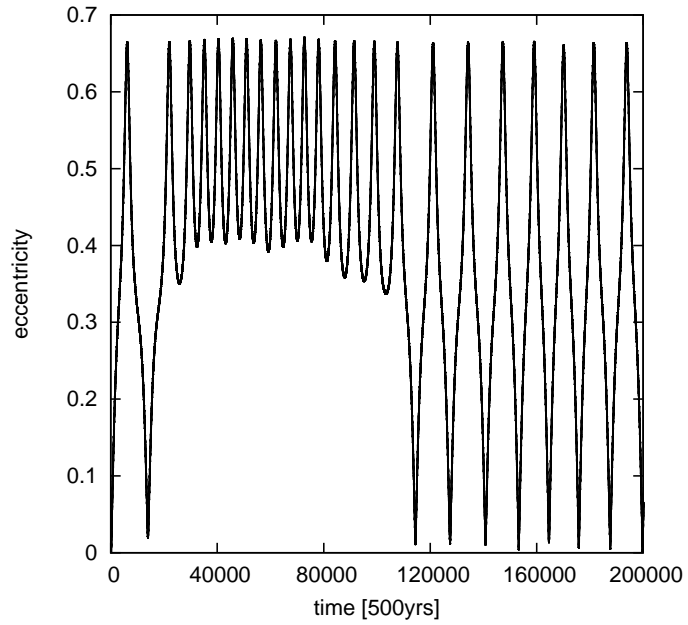


Figure 4: Same as Fig. 1 but for 100 Myrs

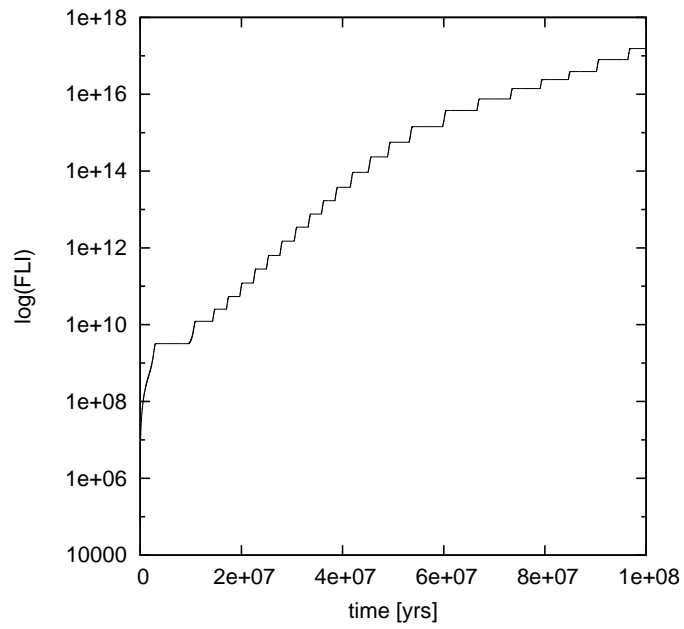


Figure 5: FLI stability plot for a test-planet at 1 au.

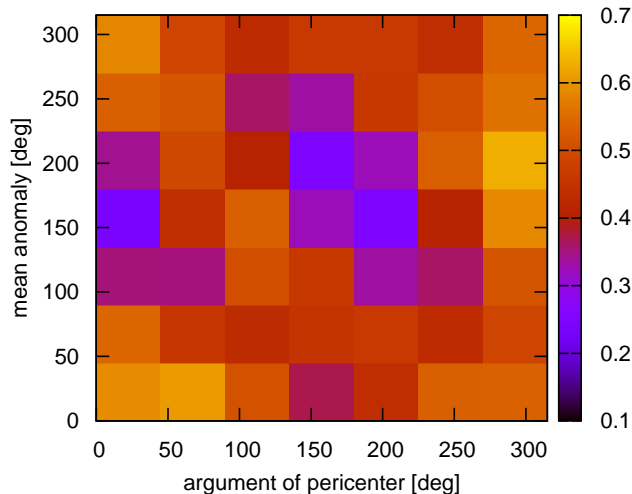


Figure 6: Maximum eccentricity of a test-planet at 1 au for various Jupiter-Saturn configurations. a_{Saturn} was fixed to 8.7 AU and its relative position to Jupiter was changed by varying Saturn’s mean anomaly and argument of peri-center. Different colors indicate different values of max-e for the test-planet at 1 AU (according the color scale).

circular motion with only small fluctuation and no secular variations (blue line in Fig. 7). This result shows again the important interplay of Venus and Earth which was also found in PL08a, where the presence of Earth helped to decrease Venus’ eccentricity to the observed value.

It is known that the orbits of Venus and Earth are connected due to a high order MMR (for details see e.g. Bazso et al., 2010). Nevertheless, it is questionable if the 13:8 MMR is also important for the damping of the eccentricity in the area affected by the secular perturbation. To check this, we performed similar computations as shown in Fig. 7 for test-planets between 0.9 and 1.1 au, and compared the max-e values of the different systems. The results are summarized in Fig. 8 where we see the secular perturbation in the Jupiter-Saturn system mainly between 0.96 and 1 au (dotted line with open squares). If we add Uranus and Neptune to the system, we can see a slight decrease in max-e for all semi-major axes ≤ 1 au (see the red line in Fig. 8). The green line, which represents the result when Mars is also included, shows clearly that Mars shifts the secular perturbation away from 1 au and consequently, the maximum eccentricity decreases at this position. Moreover, we note a significant decrease in eccentricity in this dynamical model for a planet at 0.96 au. This is the only position where the influence of Mars is stronger than that of Venus. At

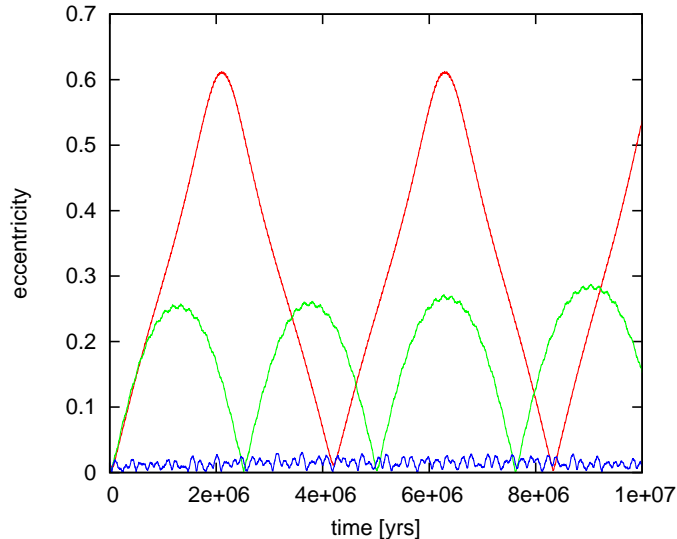


Figure 7: Evolution of the eccentricity for an orbit at 1 au in different dynamical systems.

this distance, the test planet is in 2:1 MMR with Mars. This low order MMR counteracts the secular perturbation so that the eccentricity remains low. For all other semi-major axes, we observe a strong decrease in eccentricity due to Venus.

The slight increase of max-e in the Venus-Neptune system between 0.94 and 0.96 can be explained by the interaction of two important MMRs which influence this area. These are the 2:1 MMR with Mars at 0.96 au and the 3:2 MMR with Venus at 0.948 au. In case where these MMRs overlap, chaos will arise which can be confirmed by FLI computations. Nevertheless, this might not exclude regular motion over long time-scales similar to the case of the Solar system which is chaotic but the planetary motion is stable for the life-time (i.e. the time on the main-sequence) of the Sun.

Even if we take our Solar system as reference system for this study, where the planets move in nearly the same plane, we should not ignore the possibility of mutually inclined planetary orbits.

5 Inclined Jupiter-Saturn systems

The study of a particular Jupiter-Saturn configuration (when $a_{\text{Saturn}} = 8.7$ au) for different inclinations of Saturn's orbit (from 10° to 50°) shows the perturbations of the two giant planets on the motion in the HZ, and that it depends on the mutual inclination of Jupiter and Saturn. The results of the computations are summarized in Fig. 9, where the maximum eccentricity is plotted for test-planets between 0.95 au and 1.37 au. Surprisingly, one can see low max-e values in the entire HZ for Saturns inclination up to 30° . For inclinations larger

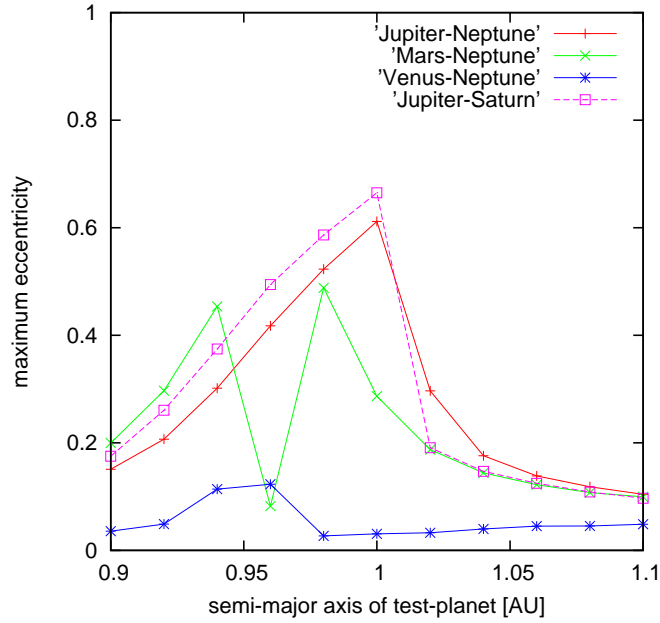


Figure 8: Maximum eccentricity for orbits in the HZ using different dynamical systems.

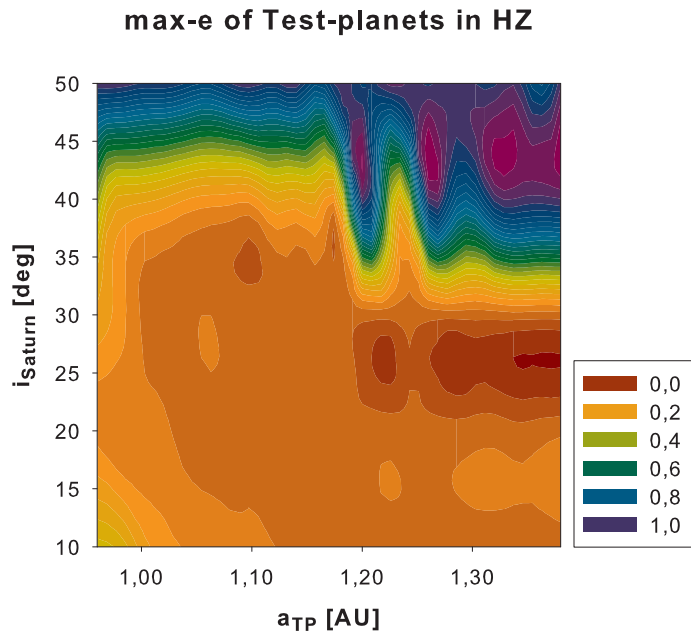


Figure 9: Max-e plot for test-planets in the HZ from 0.95 au to 1.37 au for different inclinations of Saturn (y-axis). The maximum eccentricity is given by the color code.

han that, the outer part of the HZ shows quite high eccentricities (green and blue area) as well as unstable areas (purple regions), while the inner part of the HZ ($a_{TP} < 1.2$ au) still shows low max-e values up to an inclination of 40° . If $i_{\text{Saturn}} > 45^\circ$ all orbits in the HZ have maximum eccentricities ≥ 0.8 . From this result, we follow that “Earth-like habitability” can be excluded for highly inclined Jupiter-Saturn systems (when $a_{\text{Saturn}} = 8.7$ au).

For a test-planet at 1 au, we observe the following dynamical behavior,

- (i) The nearly planar Jupiter-Saturn system shows strong variations of the eccentricity with a maximum value > 0.6 (see Fig. 1),
- (ii) For Saturn’s inclination from 10° to 40° we notice a significant decrease in max-e for this planet to values around 0.2, and
- (iii) And high inclinations of Saturn ($> 45^\circ$) lead again to high eccentricities of 0.8 for the test planet.

To get an idea about the variation of the dynamical structure, especially in the region of the significant bend, where higher eccentricity motion occurs due to secular perturbations of Jupiter and Saturn (as found in PL08a), we studied a larger region of the parameter space where the semi-major axis of the test-planet is varied between 0.6 to 1.6 au and that of Saturn changes between 8.2 and 9.8 au. The maps of Figs. 10(a-f) show the perturbations of the different Jupiter-Saturn configurations. Fig. 10a (top left panel) displays the result corresponding to the Solar system parameters. The results of the computations for inclined systems are shown in Figs. 10b (for 10°) to 10f (for 50°). Pointing our attention to the bend in Fig. 10a, which is visible up to an inclination of 30° , we observe no significant change in the shape up to $i_{\text{Saturn}} = 20^\circ$ whereas for $i_{\text{Saturn}} = 30^\circ$ (right panel in the middle), we recognize stronger perturbations due to the inclined orbit of Saturn and a change of the dynamical structure in this map. A further increase of Saturn’s inclination (bottom left panel) shows last remnants of the bend between the two horizontal blue stripes at about 8.3 au and 8.9 au, which are the locations of the 2:1 MMR and the 9:4 MMRs between Jupiter and Saturn. A comparison of the different figures shows that the spots of high eccentricity motion in the bend (see the blue-green islands in the top left panel) change significantly when increasing Saturn’s inclination. Like in Fig. 9 for $a_{\text{Saturn}} = 8.7$ au, the maximum eccentricity will decrease when increasing Saturn’s inclination. Since these perturbations result from a secular frequency associated with the precession of the perihelion of Jupiter (g_5 frequency in the Solar system), it seems that a mutual inclination of the two giant planets reduces this perturbation.

In contrast, it can be seen that the perturbations at positions of MMRs between Jupiter and Saturn are stronger in the inclined systems as the horizontal stripes in the figures indicate higher eccentricities. In the map for $i_{\text{Saturn}} = 10^\circ$ (top right panel), one can see these perturbations at about 9.6 au and 8.3 au corresponding to the 5:2 MMR and 2:1 MMR, respectively. Both stripes show a spot-like structure where the strongest perturbations are visible for test-planets with semi-major axes > 1.4 au when Jupiter and Saturn are in 2:1 MMR. An increase of i_{Saturn} to 20° leads to even stronger perturbations in this area where all test-planets with $a_{TP} > 1.3$ au escape (purple stripe) while in the map for $i_{\text{Saturn}} = 30^\circ$ (right middle panel) these test-planets indicate lower max-e

values so that fewer orbits escape than for $i_{\text{Saturn}} = 20^\circ$. The max-e map for $i_{\text{Saturn}} = 40^\circ$ does not show the perturbation at 9.6 au anymore. One can see that the dynamical structure has completely changed as the outer HZ becomes unstable (purple area) for all Jupiter-Saturn configurations. Moreover, we recognize two stripes of high eccentricities even in the inner HZ when $a_{\text{Saturn}} = 8.3$ au or 8.9 au. As can be seen from different panels, the unstable region in the outer HZ increases with Saturn’s inclination indicating that the perturbation is generated by Saturn.

6 Stability of Venus, Earth and Mars in inclined Jupiter-Saturn systems

The max-e maps of Figs. 10(a-f) allow also to determine the stability of terrestrial planets Venus (at 0.72 au), Earth (at 1 au) and Mars (at 1.52 au) when Saturn is at its actual position. The panels of various inclinations of Saturn’s orbit show that first perturbations appear for Mars when $i_{\text{Saturn}} = 20^\circ$. Mars orbit would then be in yellow-green area of Fig. 10c (left panel in the middle) which corresponds to max-e values between 0.2 and 0.3. In that case, Mars aphelion distance would be between 1.82 au and 1.98 au which is in the unstable area. For Saturns inclinations $\geq 30^\circ$, the semi-major axis of Mars is in the unstable area (purple region) which would lead immediately to an escape of this planet from the system. However, before Mars escapes, it will perturb the orbits of Earth and Venus and as a result, the dynamical behavior of all three planets change.

Numerical computations of the actual orbits of Venus, Earth and Mars in the various inclined Jupiter-Saturn configurations using the parameters of the Solar system for the planets Venus through Saturn confirmed this. A summary of these computations is shown in Fig. 11, where the maximum eccentricities of Venus, Earth and Mars are plotted for different inclinations of Saturn (from 10° to 50°). The result shows that only for an inclination of 10° of Saturn’s orbit the eccentricities of all three planets (Venus-Mars) remained small. For higher inclinations, one or several planets escaped from the system and the remaining ones have high eccentricities. In the case of $i_{\text{Saturn}} = 50^\circ$, all three terrestrial planets escaped from the system.

7 Conclusion

In this paper, we studied the dynamical behavior of test-planets moving in the water-based HZ of Sun-Jupiter-Saturn like systems. The HZ was defined to be the area between 0.95 au and 1.37 au and the test-planets were assumed to be terrestrial planets having similar conditions as Earth.

In the first part of this paper, we analyzed a particular configuration for which we knew from a previous study (PL08a) that a test-planet at 1 au would show strong variations in its eccentricity. This is the case when Jupiter orbits the Sun at 5.2 au and Saturn’s semi-major axis is changed to 8.7 au instead

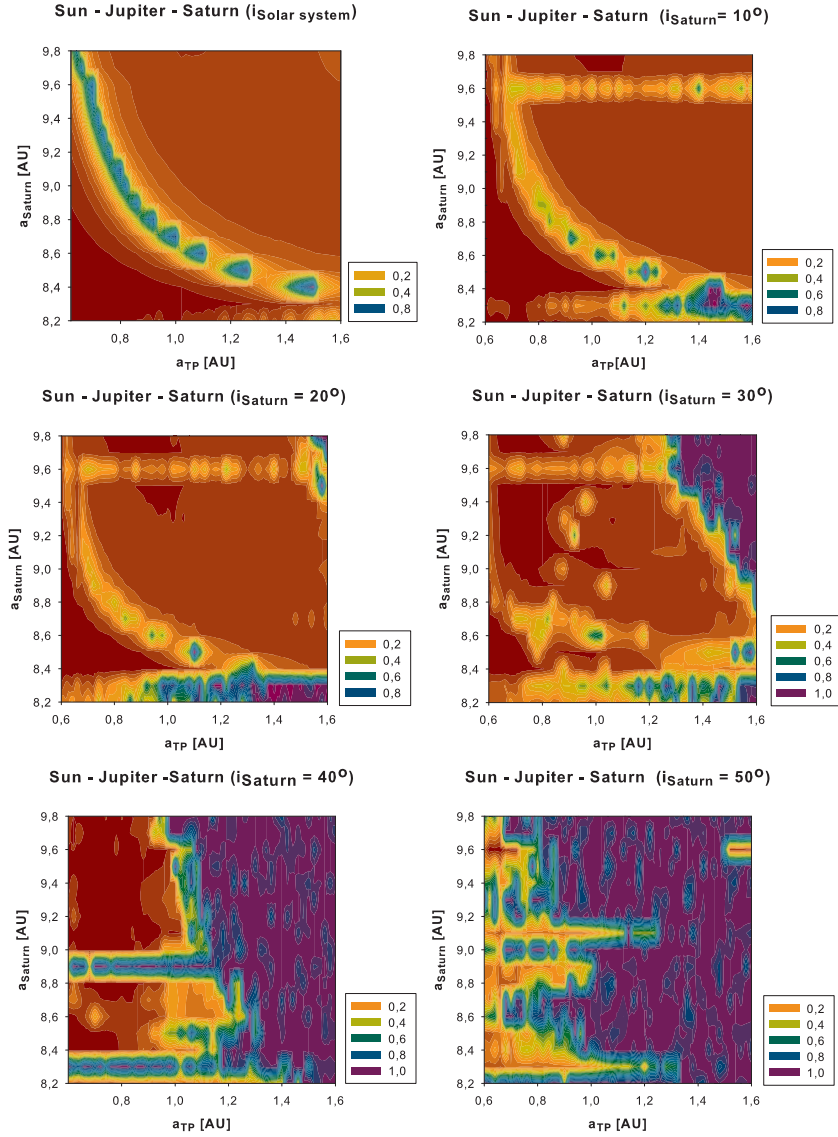


Figure 10: Max-e of test-planets in the HZ (x-axes) for different positions of Saturn (y-axes). Each map shows the maximum eccentricity for a certain inclination of Saturn: from the planar case (top left panel) to 50° (bottom right panel). Different colors denote different maximum eccentricities: from nearly circular (red areas) to unstable (purple).

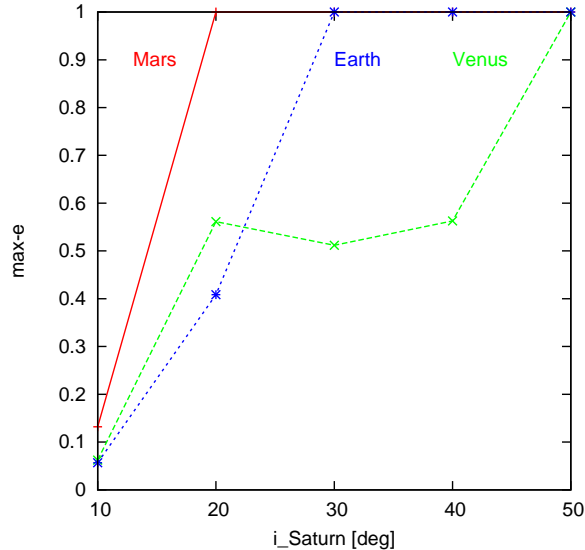


Figure 11: Maximum eccentricities of the orbits of Venus, Earth and Mars in the different Jupiter-Saturn configurations where Saturn's orbits is inclined between 10° and 50° .

of 9.53 au. This Jupiter-Saturn configuration perturbs the HZ and leads to variations in eccentricity between 0 and nearly 0.7 for a test-planet at 1 au due to a secular frequency associated with the precession of Jupiter's perihelion. In the case of an eccentric orbit, the planet might leave the HZ periodically which also depends on the size of the HZ. If the HZ is defined as the area between 0.97 au and 1.37 au (according to the works by Kasting et al., 1993 and Kopparpou et al., 2013a & b) the test-planet will exit the HZ at peri-astron for eccentricities > 0.03 and at apo-astron when $e > 0.4$. For a high-eccentric motion with $e = 0.7$, only 23% of the planets orbit will be inside the HZ. If we consider a larger HZ, i.e. between 0.95 au and 1.7 au (according to the studies by Leconte et al. 2013 and Forget & Pierrehumbert 1997) then 70% of the highly eccentric orbit would be inside the HZ.

In our study, we also checked the influence of the ice planets (Uranus and Neptune) and of the neighboring planets (Venus and Mars) where we showed that the latter ones are more important as they can decrease the eccentricity at 1 au, while Uranus and Neptune have no significant influence.

The second part of this paper analyzed the role of the mutual inclination of the two giant planets. We showed that moderate relative inclinations (up to 30°) would decrease the secular perturbation in the HZ and consequently the maximum eccentricities. In contrast, areas affected by MMRs of Jupiter and Saturn are more perturbed in the inclined systems. For higher inclinations (up to 40°) only the motion in the inner part of the HZ is stable while in the outer part it is completely chaotic. An increase of Saturn's inclination enlarges this chaotic area.

Finally, we studied the actual orbits of Venus, Earth and Mars in the various inclined Jupiter-Saturn configurations using the Solar system parameters (except for Saturn's inclination). These computations showed that for the architecture of the inner Solar system to remain stable, the inclination of Saturn's orbit can increase only up to about 10° . For inclinations $\geq 20^\circ$, we observed escapes of one or several of the three terrestrial planets and high eccentricity motion for the remaining planets. An inclination of Saturn of 50° for Saturn's orbit removed all terrestrial planets from the system.

This study shows that the planets of the Solar system have to move nearly in the same plane to ensure low-eccentricity orbits for the terrestrial planets which is probably necessary for the habitability of Earth.

Acknowledgments The author would like to thank the Austrian Science Fonds FWF for financial support of this work (projects P22603-N16 and S11608-N16).

References

- Bazso, A., Dvorak, R., Pilat-Lohinger, E., Eybl, V., Lhotka, Ch.: 2010, *CeMDA*, **107**, 57
- Chambers, J.E.: 1999, *MNRAS*, **304**, 793
- Eggl, S., Pilat-Lohinger, E., Georgakarakos, N., Gyergyovits, M., Funk, B. : 2012, *ApJ*, **752**, 74
- Eggl, S., Pilat-Lohinger, E., Funk, B., Georgakarakos, N., Haghighipour, N.: 2013, *MNRAS*, **428**, 3104
- Forget, F., Pierrehumbert, R.T.: 1997, *Science*, **278**, 1273
- Froeschlé, C.: 1984, *CMDA*, **34**
- Froeschlé, C., Lega, E., Gonczi, R.: 1997, *CMDA*, **67**, 41
- Gehman, C.S., Adams, F.C., Laughlin, G.: 1996, *PASP*, **108**, 1018
- Jones, B.W., Sleep, P.N. : 2002, *A&A*, **393**, 1015
- Jones, B.W., Underwood, D.R., Sleep, P.N.:2005, *ApJ*, **622**, 1091
- Kasting, J.F., Whitmire, D.P., Reynolds, R.T.: 1993, *Icarus*, **101**, 108.
- Kopparapu, R.K., Ramirez, R., Kasting, J.F., Eymet, V., Robinson, T.D, Mahadevan, S., Terrien, R.C., Domagal-Goldman, S., Meadows, V., Deshpande R.: 2013a, *ApJ*, **765**, 131
- Kopparapu, R.K., Ramirez, R., Kasting, J.F., Eymet, V., Robinson, T.D, Mahadevan, S., Terrien, R.C., Domagal-Goldman, S., Meadows, V., Deshpande R.: 2013b, *ApJ*, **770**, 82
- Laskar, J. 1990, *Icarus*, **88**, 266
- Lecointe, J., Forget, F., Charnay B., Wordsworth, R., Pottier, A.: 2013, *Nature*, **504**, 268
- Levison, H.F., Morbidelli, A., Tsiganis, K., Nesvorny, D., Gomes, R.: 2011, *AJ*,

142, 152

Menou, K., Tabachnik, S.: 2003, *ApJ*, **583**, 473

Mischna, M.A., Kasting, J.F., Pavlov, A., Freedman, R.: 2000, *Icarus*, **145**, 546

Morbidelli, A., Tsiganis, K., Crida, A., Levison, H.F., Gomes, R.: 2007, *AJ*, **134**, 1790

Murray, C.D., Dermott, S.F. 1999, *Solar System Dynamics*, Cambridge University Press

Pilat-Lohinger, E., Süli, Á., Robutel, P., Freistetter, F.: 2008a, *ApJ*, **681**, 1639

Pilat-Lohinger, E., Robutel, P., Süli, Á., Freistetter, F.: 2008b, *CeMDA*, **102**, 83

Robutel, P., Gabern, F.: 2006, *MNRAS*, **372**, 1463

Sándor, Zs., Süli, A., Érdi, B., Pilat-Lohinger, E., Dvorak, R.: 2007, *MNRAS*, **375**, 11495

Tsiganis, K., Gomes, R., Morbidelli, A., Levison H.F.: 2005, *Nature*, **435**, 459

Williams, D.M., Pollard, D: 2002, *IJAsB*, **1**, 61

